Dynamic scaling in one-dimensional cluster-cluster aggregation

E. K. O. Hellén,[1] T. P. Simula,[1] and M. J. Alava[1,2]
[1]*Laboratory of Physics, Helsinki University of Technology, P.O. Box 1100, FIN-02015 HUT, Finland*
[2] *NORDITA, Blegdamsvej 17, DK-2100 Copenhagen, Denmark*
(Received 16 May 2000)

We study the dynamic scaling properties of an aggregation model in which particles obey both diffusive and driven ballistic dynamics. The diffusion constant and the velocity of a cluster of size s follow $D(s)\sim s^{\gamma}$ and $v(s)\sim s^{\delta}$, respectively. We determine the dynamic exponent and the phase diagram for the asymptotic aggregation behavior in one dimension in the presence of mixed dynamics. The asymptotic dynamics is dominated by the process that has the largest dynamic exponent with a crossover that is located at $\delta=\gamma-1$. The cluster size distributions scale similarly in all cases but the scaling function depends continuously on γ and δ. For the purely diffusive case the scaling function has a transition from exponential to algebraic behavior at small argument values as γ changes sign, whereas in the drift dominated case the scaling function always decays exponentially.

PACS number(s): 64.60.Cn, 05.40.−a, 82.20.Mj, 82.70.Dd

I. INTRODUCTION

Both reaction- and diffusion-limited cluster-cluster aggregation (DLCA) have been successfully used to understand the dynamics of colloidal aggregation [1]. These models predict well both the structure of aggregates and the growth behavior in dilute particle suspensions as long as the dynamics is dominated by Brownian diffusion. As the growth of the aggregates proceeds the sedimentation of clusters due to gravitation becomes more pronounced, altering the growth mechanism and cluster structure. This was recently observed in experiments [2].

The purpose of this paper is to study dynamic scaling in one-dimensional cluster-cluster aggregation in the presence of a competition between diffusion and drift. We show that the dynamics at long times is dominated by the aggregation process, which by itself would lead to the fastest growth. The conventional mean-field theory gives the correct dynamic exponent for the field-dominated case but fails when diffusion dominates. The mean-field theory also predicts that the scaling function of the cluster size distribution in the diffusive (driven) case will drastically change when γ (δ) changes sign. Such a transition is observed for the diffusive case but not for the driven one. The dynamic phase diagram shows four different regions depending on the relative rates of the diffusion and drift.

The paper is organized as follows. Section II introduces the model and describes the algorithm used in simulations. In Sec. III the dynamic scaling is studied using the mean-field rate equation approach. The mean-field results are compared to simulations in Sec. IV. Section V concludes the paper with a discussion.

II. MODEL

The field-driven cluster-cluster aggregation (FDCA) model is defined on a one-dimensional lattice with periodic boundary conditions, for simplicity. Initially particles are distributed randomly on a lattice of L sites up to a concentration ϕ. Sites connected via nearest neighbor occupancy are identified as belonging to the same cluster. The diffusion coefficient of a cluster of size s takes the form $D(s)=D_1 s^{\gamma}$, where γ is the diffusion exponent and D_1 a non-negative constant. The clusters are also driven in one direction with a size dependent drift velocity $v(s)=v_1 s^{\delta}$, which defines the field exponent δ.

In simulations a cluster is selected randomly and the time is incremented by $N(t)^{-1}\Omega_{\max}^{-1}$, where $N(t)$ is the number of clusters at time t and $\Omega_{\max}$ is the maximum mobility of any of the clusters in the system at that time. The cluster mobility is defined as $\Omega(s)=C_v s^{\delta}+2C_D s^{\gamma}$ where C_v and C_D are non-negative constants. The choice $C_v=0$ gives normal DLCA. The cluster is moved only if $x<\Omega(s)/\Omega_{\max}$, where x is a uniformly distributed random number in the interval [0,1]. The step is taken along (against) the field with probability $p(q)$, where $p=(C_v s^{\delta}+C_D s^{\gamma})/\Omega(s)$ and $q=1-p$. If after the move two clusters are in contact, they are irreversibly aggregated together. Note that time is increased for each attempted move.

Figure 1 shows an example of the dynamics when either the diffusion [Fig. 1(a)] or the drift [Fig. 1(b)] dominates the large-time aggregation behavior. The diffusion and field exponents are chosen in such a way that at large times the largest clusters are the most mobile ones. In Fig. 1(b), notice the clear breaking of the reflection symmetry in the cluster dynamics as the drift begins to dominate. Similar behavior is visible in the early-time dynamics of the diffusion-dominated case.

III. SCALING ANALYSIS

Before considering any specific aggregation rules let us first present the well-known mean-field approach. We want to compare different dynamical processes in order to find the dominating aggregation mechanisms. Denote the number of clusters of size s per site at time t by $n_s(t)$ and the mean cluster size by $S(t)$. The mean-field description of irreversible aggregation, which neglects spatial correlations, is given by Smoluchowski's equation [3]

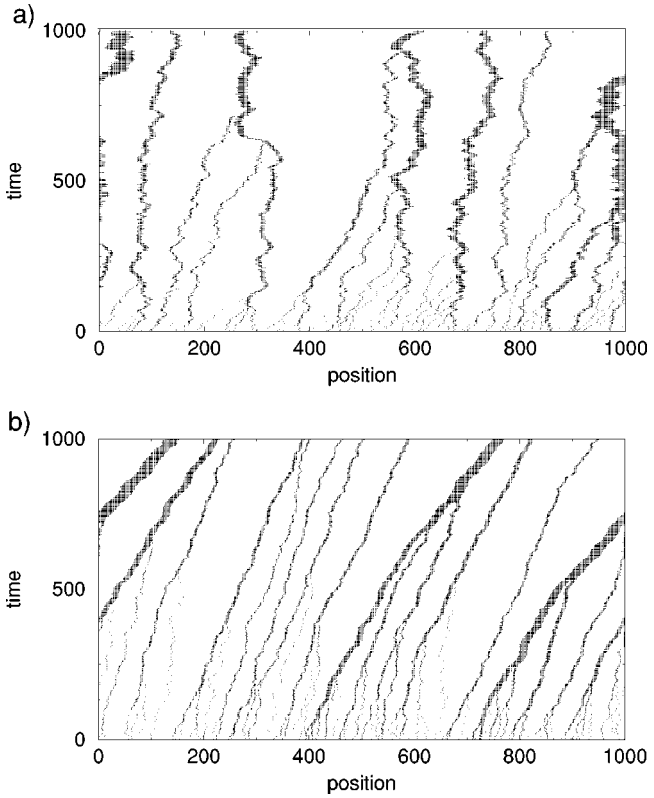

FIG. 1. An example of the dynamics in FDCA for $\phi=0.1$, (a) $\gamma=0.5$, $\delta=-1.0$, and (b) $\gamma=-1.0$, $\delta=0.5$. System size $L=1000$. The time scales are normalized differently.

$$\frac{dn_s}{dt}=\frac{1}{2}\sum_{i+j=s}K(i,j)n_in_j-\sum_{i=1}^{\infty}K(i,s)n_in_s, \qquad (1)$$

where the reaction kernel $K(i,j)$ describes the rate at which clusters of size i and j aggregate. It is assumed to be a homogeneous function $K(ai,aj)=a^{\lambda}K(i,j)$ with $K(i,j)\sim i^{\mu}j^{\lambda-\mu}$ for $i\ll j$. Kernels are classified by μ [4]: $\mu>0$ (class I), $\mu=0$ (class II), and $\mu<0$ (class III). Independent of the class the solution scales for mass conserving systems as $n_s(t)=S(t)^{-2}f(s/S(t))$. In class I the aggregation is dominated by the collisions of large clusters with large ones whereas the dominant contribution in class III comes from the reactions between large and small clusters. In class II these two processes are equally important. The class III processes can be identified from the form of the scaling function since in classes I and II $f(x)\sim x^{-\tau}$ but in class III $f(x)\sim\exp(-x^{-|\mu|})$ as $x\to 0$ [4].

Here we concentrate on the scaling function, on the polydispersity exponent τ, and on the dynamic exponent z describing the growth of the mean cluster size: $S(t)\sim t^z$. The polydispersity exponent in the mean field (MF) is easily found to be $\tau_{\rm MF}=1+\lambda$ in class I. Predicting it for class II processes is still a challenge [5]. However, for all nongelling systems, i.e., $\lambda\leqslant 1$, the dynamic exponent is related to the homogeneity exponent λ as $z_{\rm MF}=1/(1-\lambda)$ [4].

The upper critical dimension, above which the mean-field theory is exact, may be calculated once the reaction kernel is known [6]. Consider for a moment the aggregation of clusters of fractal dimension d_f in d dimensions. For a DLCA kernel $K_D(i,j)\sim(i^{1/d_f}+j^{1/d_f})^{d-2}(i^{\gamma}+j^{\gamma})(d\geqslant 2)$, the mean-field theory is not exact in any finite dimension [6] but the deviations are already negligible in $d=3$ [7]. In the driven case, if diffusion and velocity fluctuations are neglected, clusters move ballistically. The collision probability of two clusters is proportional to the product of the mutual cross section of the clusters and the velocity difference between clusters, $K_v(i,j)\sim(i^{1/d_f}+j^{1/d_f})^{d-1}|i^{\delta}-j^{\delta}|$. Thus in the mean-field description the driven system in d dimensions has similar scaling properties as the diffusive one in $d+1$ dimensions and therefore the upper critical dimension is infinite for both.

If both diffusion and drift are present the faster dynamics, as measured by the associated dynamic exponent, could be expected to dominate. This is verified by the simulation results, discussed in the next section. Thus it is adequate to consider the two dynamic processes separately. For example, in one dimension the scaling properties of K_v necessitate that $\lambda=\delta$ together with $\mu=\delta$ for $\delta<0$ (class III) and $\mu=0$ for $\delta\geqslant 0$ (class II). Thus the scaling function should drastically change as δ changes its sign. In one dimension the collision cross section is independent of the cluster sizes. Thus the above scaling analysis is directly applicable to the diffusion-limited case, too, and there should be a similar transition between the classes III and II at $\gamma=0$.

In one dimension the scaling properties of the reaction kernels together with $z_{\rm MF}=1/(1-\lambda)$ give the mean-field dynamic exponent in the diffusive and driven cases as $z_{\rm MF}=1/(1-\gamma)$ and $z_{\rm MF}=1/(1-\delta)$, respectively. The strong fluctuations are responsible for the fact that the correct exponent is $z=1/(2-\gamma)$ in the diffusive case [8,9]. The dynamic exponent may, on the other hand, be obtained more simply by considering the two length scales coming from the two dynamical processes: the diffusive length scale $l_D\sim\sqrt{Dt}$ and the ballistic one $l_v\sim vt$. Naturally, the average cluster size is proportional to the dominant length scale, i.e., $S(t)\sim l$, which together with $D(s)\sim s^{\gamma}$ and $v(s)\sim s^{\delta}$ results in $z=1/(2-\gamma)$ and $z=1/(1-\delta)$ for the diffusion- and drift-dominated cases, respectively. The simulation results presented in Sec. IV confirm these arguments. Thus the Smoluchowski approach predicts the correct dynamic exponent for the driven case even in one dimension. If both diffusion and drift are present $z=\max\{1/(2-\gamma),1/(1-\delta)\}$ with the crossover at $\delta=\gamma-1$.

The average cluster size at the crossover can be estimated by comparing the pairing time (the time required for $S\to 2S$) due to diffusion, $t^D_{\rm agg}$, to that due to drift, $t^v_{\rm agg}$. In the diffusive case the pairing time can be obtained by considering a random walk on a coarse-grained system with the lattice constant set equal to the average cluster radius R [10]. In one dimension the cluster density on the lattice is $\rho(t)=N(t)/V=\phi$, where the volume $V=L/R$. A cluster travels a distance of its own radius diffusively in time R^2/D. As it takes on the average ρ^{-2} steps to pair up, $t^D_{\rm agg}=R^2/(D\rho^2)$.

For driven clusters the variation in cluster velocities is the relevant parameter. Therefore the pairing time is of order $t^v_{\rm agg}=R/(\sigma_v\rho)$, where $\sigma_v=\sqrt{\langle v^2\rangle-\langle v\rangle^2}$ is the standard deviation of the cluster velocities. It can be calculated from the velocity distribution $p(v)=sn_s|\partial s(v)/\partial v|$, which gives $\sigma_v\approx v_1S^{\delta}\sqrt{I_2-I_1^2}$, where $I_{\alpha}=\int dx x^{\delta\alpha+1}f(x)$ and the approxi-

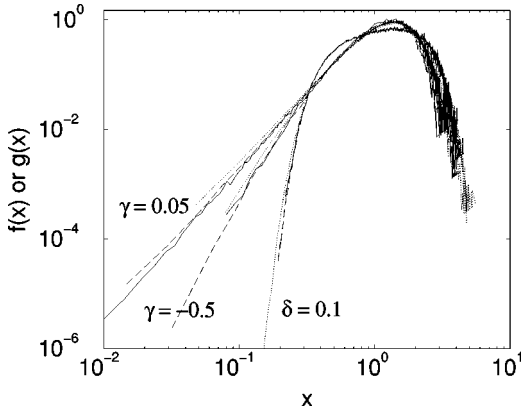

FIG. 2. The numerically obtained scaling functions as a function of the scaling variable $x=s/S(t)$ for DLCA (γ) and FDCA (δ) at times $10^4(\cdots)$, 10^5 (– –), and 9×10^5 (—). System sizes and number of realizations are $(5\times10^5,50)$, $(5\times10^5,1000)$, and $(2\times10^6,2000)$ for $\gamma=-0.5$, $\gamma=0.05$, and $\delta=0.1$, respectively.

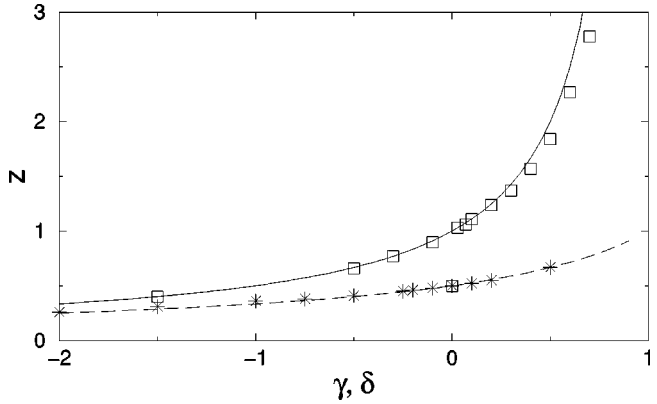

FIG. 3. Dynamic exponent from simulations as a function of either the diffusion exponent γ (*) or the field exponent δ (□). The solid line is given by $1/(1-\delta)$ and the dashed one by $1/(2-\gamma)$.

mation comes from replacing the sum by an integral. The proportionality constant $A=\sqrt{I_2-I_1^2}$ has to be determined numerically from simulations since calculating it would require knowledge of the whole scaling function. The crossover takes place as $t^v_{\rm agg}\approx t^D_{\rm agg}$ which gives the average cluster size at the crossover as

$$S_{\rm cross}\approx\left(\frac{2D_1\phi}{Av_1r_0}\right)^{1/(\delta-\gamma+1)}, \tag{2}$$

where r_0 is the elementary particle radius.

IV. SIMULATIONS

In simulations the system sizes range from 5×10^5 to 2×10^6, the data are averaged over 50–2000 realizations, the concentration is usually at $\phi=0.1$, and random initial conditions are used. Neither the initial conditions nor the concentration have any effect on the asymptotic dynamic scaling properties as was verified by simulations. The time scale is fixed by setting $C_D=1$ for DLCA and $C_v=1$ for FDCA if not otherwise mentioned. The mean cluster size is calculated using both the number ($k=1$) and weight averages ($k=2$),

$$S_k(t)=\sum_{s=1}^{\infty}s^k n_s(t)\Big/\sum_{s=1}^{\infty}s^{k-1}n_s(t). \tag{3}$$

Both averages scale similarly and the number average is used in all the figures following. In order to ensure that the scaling regime is reached the dynamic exponent is calculated using the method of consecutive slopes [11].

We first consider purely diffusive dynamics, i.e., $C_v=0$. We obtain an excellent scaling for the cluster size distribution using the scaling form $n_s(t)=S(t)^{-2}f(s/S(t))$ (Fig. 2) and the known [8,9] result for the dynamic exponent $z=1/(2-\gamma)$ (Fig. 3).

The decay of the scaling function near $x=0$ depends on the sign of γ and there is a transition from class III ($\gamma<\gamma_c$) to class II ($\gamma\geqslant\gamma_c$) at $\gamma_c=0$ in accordance with the mean-field analysis. However, the transition between the algebraic and nonalgebraic decay of the scaling function is plagued by strong crossover effects. This is illustrated in Fig. 4 where the scaling functions are presented for several values of the diffusion exponent. The crossover behavior is in excellent agreement with mean-field theory, according to which the kernels in classes I and III show typical class II behavior for intermediate x values: $\exp(-1/|\mu|)\ll x\ll 1$ [4]. In our case $\mu=\gamma$ and the intermediate x region is presented by horizontal lines in Fig. 4. The dynamics for $\gamma=0$ can be solved exactly to establish that DLCA belongs to class II at γ_c. The exact result for the cluster size distribution is $n_s(t)=\exp(-T)[I_{s-1}(T)-I_{s+1}(T)]$, where $T=4D_1t$ and $I_s(T)$ is the modified Bessel function [12]. This gives $f(x)\simeq x\exp(-Cx^2)\sim x$ $(x\to0)$, where the constant C depends on the average used to calculate the mean cluster size.

As the scaling function decays faster than a power law in class III the polydispersity exponent τ is well defined only for $\gamma\geqslant0$. Although the statistics is insufficient for a direct determination of the relationship $\tau(\gamma)$, the fits to the scaling

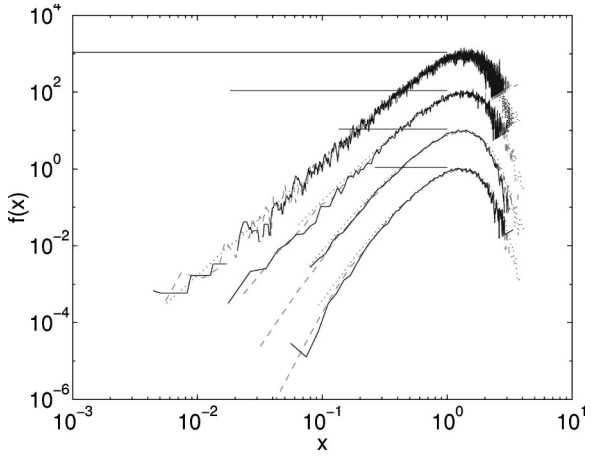

FIG. 4. The scaling functions as a function of the scaling variable for DLCA for $\gamma=-0.05$, -0.25, -0.50, -0.75 (from top to bottom) at the times 10^4 $(\cdots)$, 10^5 (– –), and 9×10^5 (—). System size $L=5\times10^5$ and data are averaged over 25 runs except for $\gamma=-0.05$ (491 runs). Horizontal lines show the crossover region $\exp(1/\gamma)\leqslant x\leqslant1$ where the scaling functions show typical class II behavior. The data for various γ values have been shifted in the vertical direction to make the figure clearer.

function show that τ increases monotonically with increasing γ so that $\tau=0$ at about $\gamma\approx 0.7$. The scaling theory states that for class II $n_s(t)\sim s^{-\tau}t^{-w}$ for $1\ll s\ll S$ and $t\to\infty$ with the scaling relation $w=(2-\tau)z$ [4]. The exponent w can be obtained more accurately from simulations than τ. A careful analysis of the data shows that w is roughly a constant, $w\approx 1.50\pm 0.05$, for $\gamma\in[0,0.5]$. However, w cannot be independent of γ since necessarily $w\geq z$, which diverges when $\gamma\to 2$. Approximating $w\approx 1.50$ near $\gamma=0$ leads to $\tau(\gamma)\approx 1.50\gamma-1.00$, which is zero at $\gamma_0\approx 0.67$ (compare with the actual result above). This approximation is consistent with the exact value $\tau(0)=-1$ [12].

Note that the point $\gamma_0\approx 0.7$ at which the cluster size distribution changes from a nonmonotonic function to a monotonic one is not the same as the transition point between the classes $\gamma_c=0$. In the literature it has been argued that in two and three dimensions γ_c is negative, but these arguments rely on the fact the cluster size distribution would change to a nonmonotonic function at the same point [13]. As this is clearly not the case in one dimension it is highly probable that $\gamma_c=0$ in higher dimensions, too.

The corresponding FDCA simulations are done using $C_D=0$. Figure 3 shows for this case also the dynamic exponent as a function of the field exponent together with the mean-field prediction. The agreement is excellent except for $\delta>0.3$, for which values the asymptotic regime has not been reached. $\delta=0$ is a special point: all the clusters move with the same velocity but the algorithm itself causes intrinsic diffusion, resulting in the standard random walk value $z(\delta=0)=1/2$.

As in the purely diffusive case, the cluster size distribution exhibits scale invariance $n_s(t)=S(t)^{-2}g(s/S(t))$ but now with a bell-shaped scaling function $g(x)\sim\exp(-x^{-|\mu|})$ as $x\to 0$ (see Fig. 2). Thus FDCA belongs to class III. No indication of belonging to class II is seen in the range $-1.5\leq\delta\leq 0.7$, in contradiction with the result of mean-field theory. The absence of the transition shows that although the mean-field analysis gives the correct dynamic exponent it fails in the case of the scaling function. This is not surprising since the spatial fluctuations expected to be important in low dimensions are completely neglected in Eq. (1). Furthermore, for $\delta>0$ the probability for collisions of large clusters with large ones is relatively small compared to large-small collisions, since the decisive factor is the velocity difference, not the high mobility of large clusters.

The case $\delta=\gamma=0$ of FDCA is, interestingly enough, related to a driven diffusive Ising system (DDS). The low temperature coarsening in an Ising chain with conserved magnetization and subject to a small external force can be mapped almost exactly to the diffusion of domains with a size-independent diffusion constant [14]. The fact that the mapping is not quite one to one is reflected in the behavior of dimers in the DDS. They perform long-range hopping, which results in another characteristic length scale in the problem [15]. As a consequence, the domain length distribution does not obey the usual dynamic scaling for small cluster sizes as it does in FDCA, although the domain size distributions are otherwise practically the same [15].

Figure 5 shows the crossover from diffusion-dominated growth to field-dominated growth for three different concentrations. Estimating the unknown parameter A in Eq. (2) using the scaling function of diffusion-limited aggregation for $\gamma=-0.5$ gives $A\approx 0.2$. Equation (2) gives the crossover sizes 3, 4, and 10 for concentrations $\phi=0.05$, 0.1, and 0.5, respectively. These values agree reasonably well with the simulations as can be seen from Fig. 5.

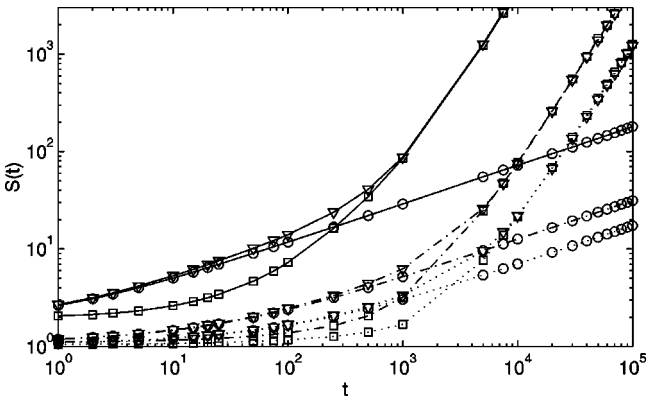

FIG. 5. Average cluster size for various mobilities and concentrations for $\gamma=-0.5$ and $\delta=0.5$ in the diffusive $C_D=1$, $C_v=0$ ($\bigcirc$), driven $C_D=0$, $C_v=0.05$ ($\square$), and driven diffusive $C_D=1$, $C_v=0.05$ (∇) cases. Data are averaged over 50 runs and system sizes are 10^6, 5×10^5, and 10^5 for concentrations $\phi=0.05$ ($\cdots$), 0.1 ($-\cdot$), and 0.5 (—), respectively.

V. DISCUSSION

The results of our study are summarized in Fig. 6, which shows the dynamic phase diagram with four different regions. The aggregation is dominated by the field or the diffusion. At the phase boundary $\delta=\gamma-1$ the two processes give the same dynamic exponent. It is unclear which one of the aggregation mechanisms determines the asymptotic scaling behavior at the boundary. The diffusive phase is split into two subphases according to the dominating aggregation mechanism. The dynamics may also be so fast that the system gels in a finite time.

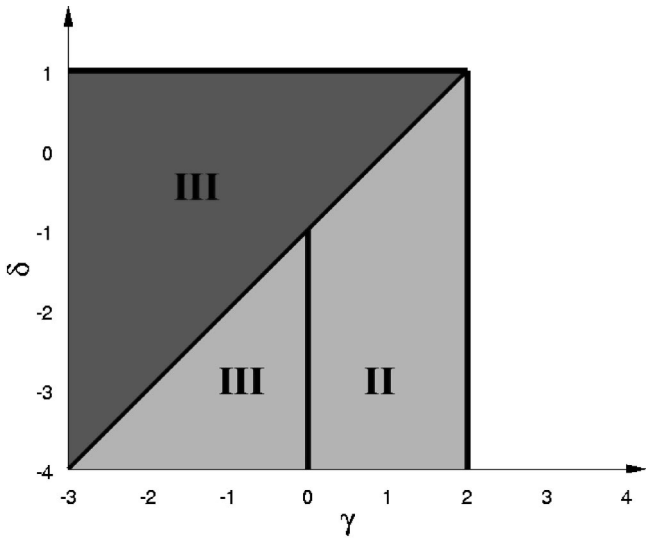

FIG. 6. The phase diagram in one dimension. Roman numbers indicate the class of the aggregation process. Aggregation is dominated by diffusion (light gray), the field (dark gray), or a gelation transition (white).

Although this paper has considered $d=1$, we can also discuss the $d>1$ case. Here, complications arise because the clusters may have a fractal structure. For field-driven aggregation the clusters will in any case become anisotropic with a preferred orientation in the field direction. We believe both of these complications affect only the phase boundaries of the dynamic phase diagram but leave its general structure invariant if temporal scaling can be assumed. One particular issue is the existence of a field-dominated phase with a scaling function belonging to class II. Comparison of the mean-field approach and simulations in higher dimensions is left for a forthcoming study. The exact location of the phase boundaries would be an interesting problem also when it comes to applications to experiments.

In conclusion, we have studied one-dimensional driven diffusive cluster-cluster aggregation. We have shown how the scaling function depends on the cluster mobilities with diffusive or ballistic dynamics, or both. For the field-dominated case the dynamic exponent can be obtained from simple mean-field calculations, which together with the simulation results may be used to obtain the phase boundaries in the dynamic phase diagram. This shows four different phases in the aggregation depending on the relative strengths of the diffusion and the field.

[1] P. Meakin, Phys. Scr. **46**, 295 (1992).
[2] C. Allain, M. Cloitre, and F. Parisse, J. Colloid Interface Sci. **178**, 411 (1996).
[3] M. von Smoluchowski, Z. Phys. **17**, 585 (1916).
[4] P. G. J. van Dongen and M. H. Ernst, Phys. Rev. Lett. **54**, 1396 (1985).
[5] S. Cueille and C. Sire, Phys. Rev. E **55**, 5465 (1997).
[6] P. G. J. van Dongen, Phys. Rev. Lett. **63**, 1281 (1989).
[7] R. M. Ziff, E. D. McGrady, and P. Meakin, J. Chem. Phys. **82**, 5269 (1985).
[8] K. Kang, S. Redner, P. Meakin, and F. Leyvraz, Phys. Rev. A **33**, 1171 (1986).
[9] S. Miyazima, P. Meakin, and F. Family, Phys. Rev. A **36**, 1421 (1987).
[10] M. Kolb, Phys. Rev. Lett. **53**, 1653 (1984).
[11] A.-L. Barabási and H. E. Stanley, *Fractal Concepts in Surface Growth*, 1st ed. (Cambridge University Press, Cambridge, UK, 1995).
[12] J. L. Spouge, Phys. Rev. Lett. **60**, 871 (1988).
[13] P. Meakin, T. Vicsek, and F. Family, Phys. Rev. B **31**, 564 (1985).
[14] S. J. Cornell and A. J. Bray, Phys. Rev. E **54**, 1153 (1996).
[15] V. Spirin, P. L. Krapivsky, and S. Redner, Phys. Rev. E **60**, 2670 (1999).